Supplementary Materials: One-pot Bi-enzymatic Cascade Synthesis of Novel Ganoderma Triterpenoid Saponins

Te-Sheng Chang [1,+,*], Chien-Min Chiang [2,+], Tzi-Yuan Wang [3], Yu-Li Tsai [1], Yu-Wei Wu [4,5], Huei-Ju Ting [1,*] and Jiumn-Yih Wu [6,*]

Table S1. NMR spectroscopic data for GAA-G2 (in pyridine-d_5; 700MHz).

Compound			GAA-G2	
Position	type	δ_C ,	δ_H (*J* in Hz)	HMBC
GAA moiety				
1	CH2	36.2	3.12, m	H-2, H-19
			1.52, m	
2	CH2	34.7	2.56, m	H-1
			2.52, m	
3	C	215.9		H-1, H-2, H-28, H-29
4	C	46.8		H-5, H-6, H-28, H-29
5	CH	49.1	1.71, dd (13.4, 2.1)	H-1, H-6, H-19, H-28, H-29
6	CH2	30.6	2.12, m	H-5, H-7
			1.97, m	
7	CH	67.1	5.17 dd (9.8, 7.5)	H-5, H-6
8	C	161.9		H-6, H-7, H-15, H-30
9	C	140.7		H-1, H-5, H-7, H-12, H-19
10	C	38.1		H-1, H-2, H-5, H-6, H-19
11	C	199.3		H-12
12	CH2	52.1	2.88, d (16.4)	H-18
			2.64, d (16.3)	
13	C	46.3		H-12, H-17, H-18, H-30
14	C	54.2		H-12, H-15, H-16, H-18, H-30
15	CH	82.7	5.34, dd (9.4, 6.3)	H-14, H-30, **Glc1-H-1′**
16	CH2	35.7	2.50, m	H-17
			1.96, m	
17	CH	49.2?	1.81, q (10.2)	H-12, H-16, H-18, H-21, H-22
18	CH3	17.7	1.09, s	H-12, H-17
19	CH3	18.9	1.43, s	H-1, H-5
20	CH	32.9	2.16, m	H-16, H-17, H-21, H-22
21	CH3	19.6	0.91, d (5.8)	H-22
22	CH2	49.9	2.51, m	H-17, H-21
			2.18, m	
23	C	209.0		H-22, H-24, H-25
24	CH2	47.0	3.03, dd (17.6, 8.4)	H-25, H-27
			2.54, m	
25	CH	35.6	3.26, m	H-24, H-27
26	C	178.2		H-24, H-25, H-27
27	CH3	17.6	1.33, d (7.2)	H-24, H-25
28	CH3	26.8	1.07, s	H-5, H-29
29	CH3	20.9	1.07, s	H-5, H-28
30	CH3	21.9	1.46, s	H-15
Glucose 1 moiety				
1′	CH	105.0	4.86, d (7.9)	**H-15**, H-2', H-3', H-5'
2′	CH	75.2	4.01, t (8.2)	H-3' , H-5'
3′	CH	78.1	4.29, m	H-1', H-2' , H-4', H-5'
4′	CH	81.2	4.30, m	H2', H-3' , H-5', H-6', **Glc2-H-1''**
5′	CH	76.7	3.77, m	H-1', H-2', H-4', H-6'
6′	CH2	61.9	4.42 d (3.2), 2H	H-4', H-5'
Glucose 2 moiety				
1''	CH	103.0	5.88, d(3.9)	**Glc1-H-4'**, H-3''
2''	CH	74.3	4.16, dd (9.6, 3.8)	H-3''
3''	CH	75.29	4.55, m	H-1'', H-2'', H-4''
4''	CH	71.8	4.13, t (9.4)	H-3'', H-6''
5''	CH	75.30	4.55, m	H-2'', H-4'', H-6''
6''	CH_2	62.6	4.52, m	H-4'', H-5''
			4.31, m	

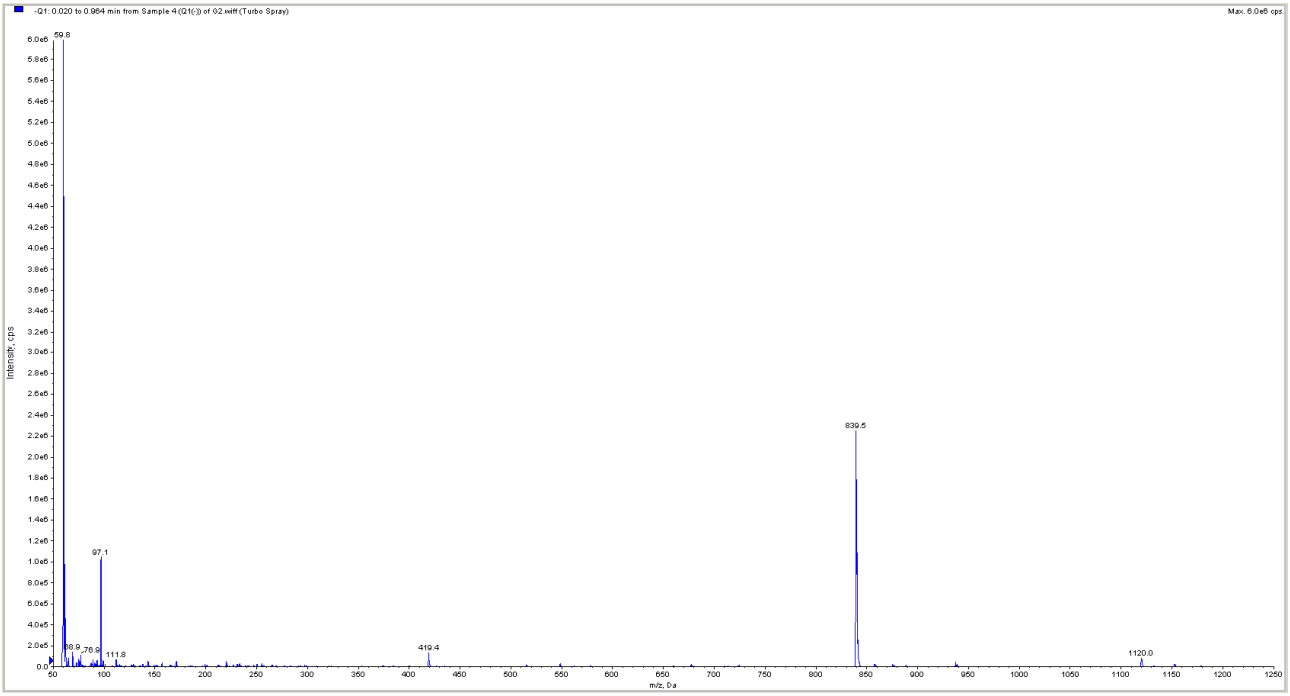

Figure S1. Mass analysis of GAA-G2 at the negative mode. A significant signal at m/z 839.5 showed the corresponding m/z signal of molecular weight 840 of GAA-diglucoside (516+180*2-18*2) at the negative mode $[GAA\text{-}G2 - H]^-$.

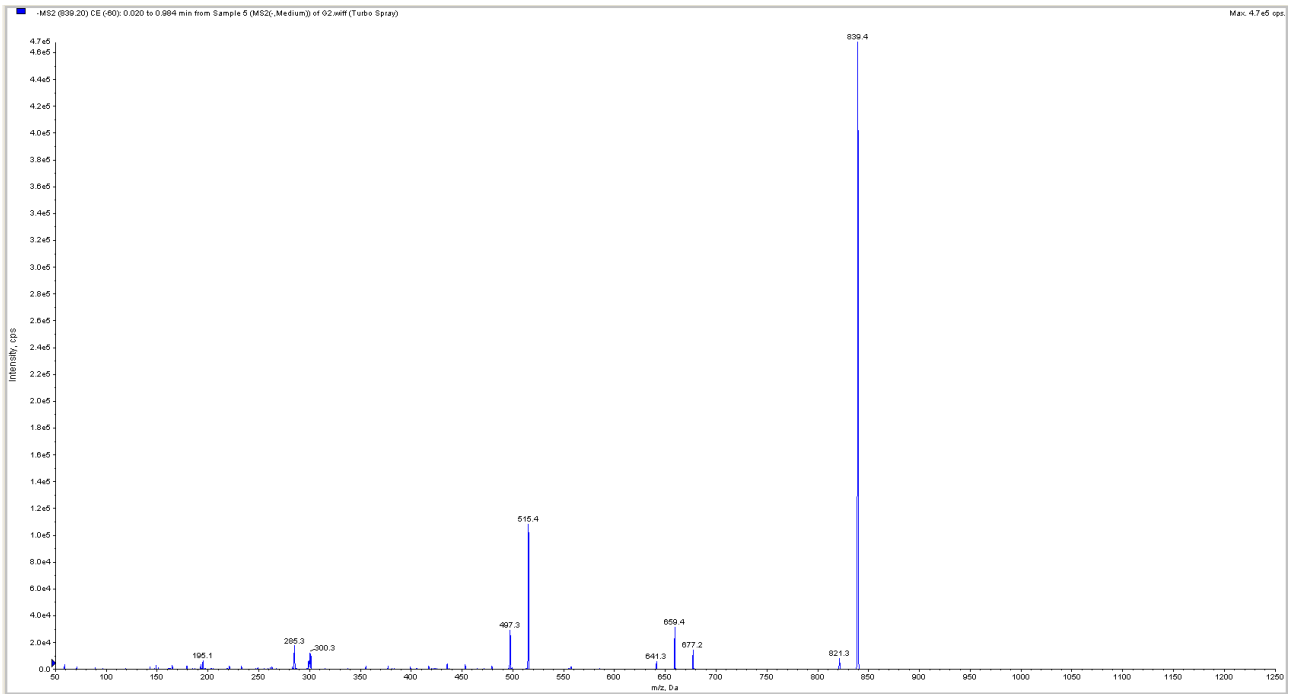

Figure S2. Mass-mass analysis of the m/z 839.5 peak of GAA-G2 at the negative mode. Two significant peaks at m/z 677.2 and 515.4 showed the corresponding m/z signals of molecular weights 678 and 516 of GAA-glucoside (516+180-18) and GAA (516) at the negative mode $[GAA\text{-}G - H]^-$ and $[GAA - H]^-$.

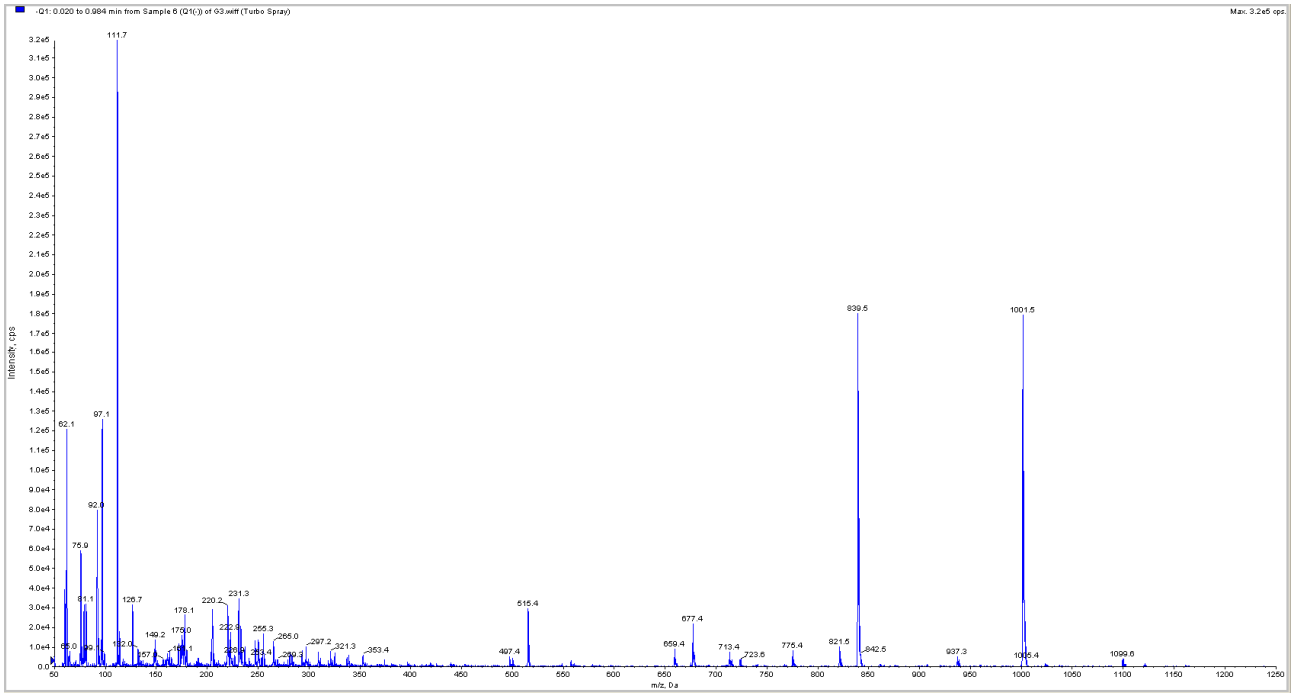

Figure S3. Mass analysis of GAA-G3 at the negative mode. A significant signal at m/z 1001.5 showed the corresponding m/z signal of molecular weight 1002 of GAA-triglucoside (516+180*3-18*3) at the negative mode $[GAA\text{-}G3 - H]^-$.

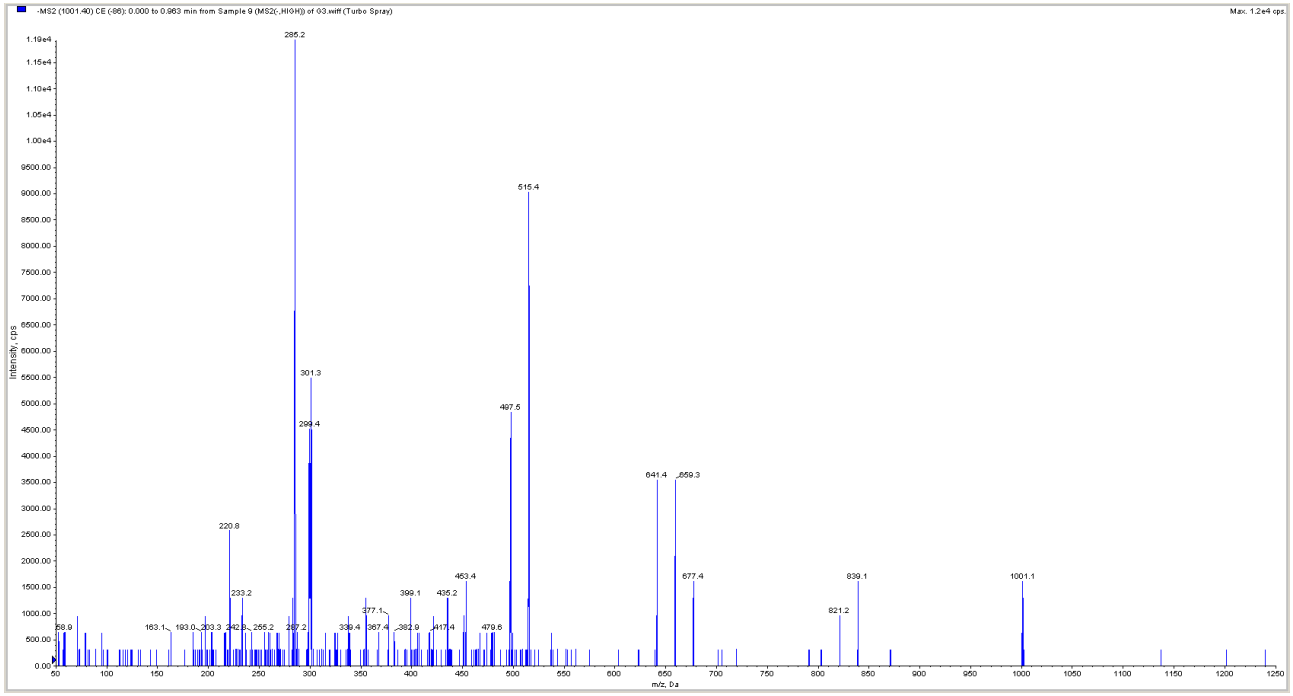

Figure S4. Mass-mass analysis of the m/z 1001.5 peak of GAA-G3 at the negative mode. Three significant peaks at m/z 839.1, 677.4 and 515.4 showed the corresponding m/z signals of molecular weights 840, 678 and 516 of GAA-diglucoside (516+180*2-18*2), GAA-glucoside (516+180-18) and GAA (516) at the negative mode $[GAA\text{-}2G - H]^-$, $[GAA\text{-}G - H]^-$ and $[GAA - H]^-$.

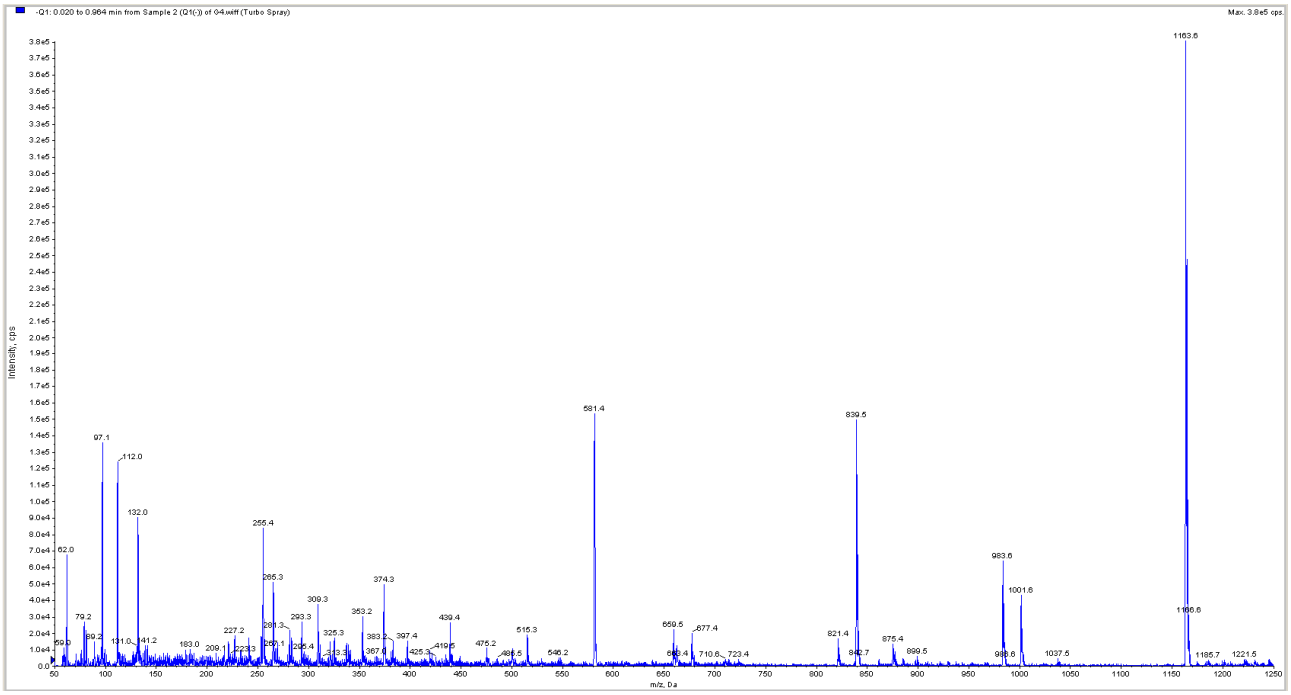

Figure S5. Mass analysis of GAA-G4 at the negative mode. A significant signal at m/z 1163.6 showed the corresponding m/z signal of molecular weight 1164 of GAA-tetraglucoside (516+180*4-18*4) at the negative mode $[GAA\text{-}G4 - H]^-$.

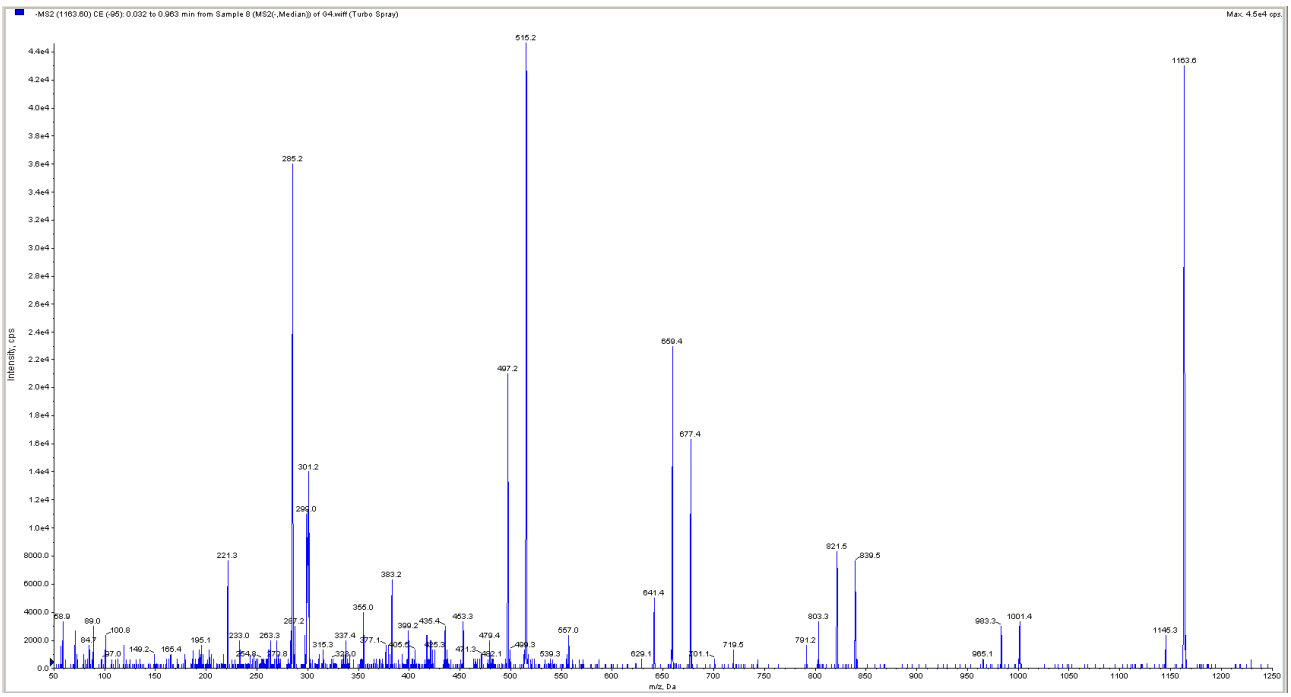

Figure S6. Mass-mass analysis of the m/z 1163.6 peak of GAA-G4 at the negative mode. Three significant peaks at m/z 1001.4, 839.5, 677.4 and 515.2 showed the corresponding m/z signals of molecular weights 1002, 840, 678 and 516 of GAA-triglucoside (516+180*3-18*3), GAA-diglucoside (516+180*2-18*2), GAA-glucoside (516+180-18) and GAA (516) at the negative mode $[GAA\text{-}3G - H]^-$, $[GAA\text{-}2G - H]^-$, $[GAA\text{-}G - H]^-$ and $[GAA - H]^-$.

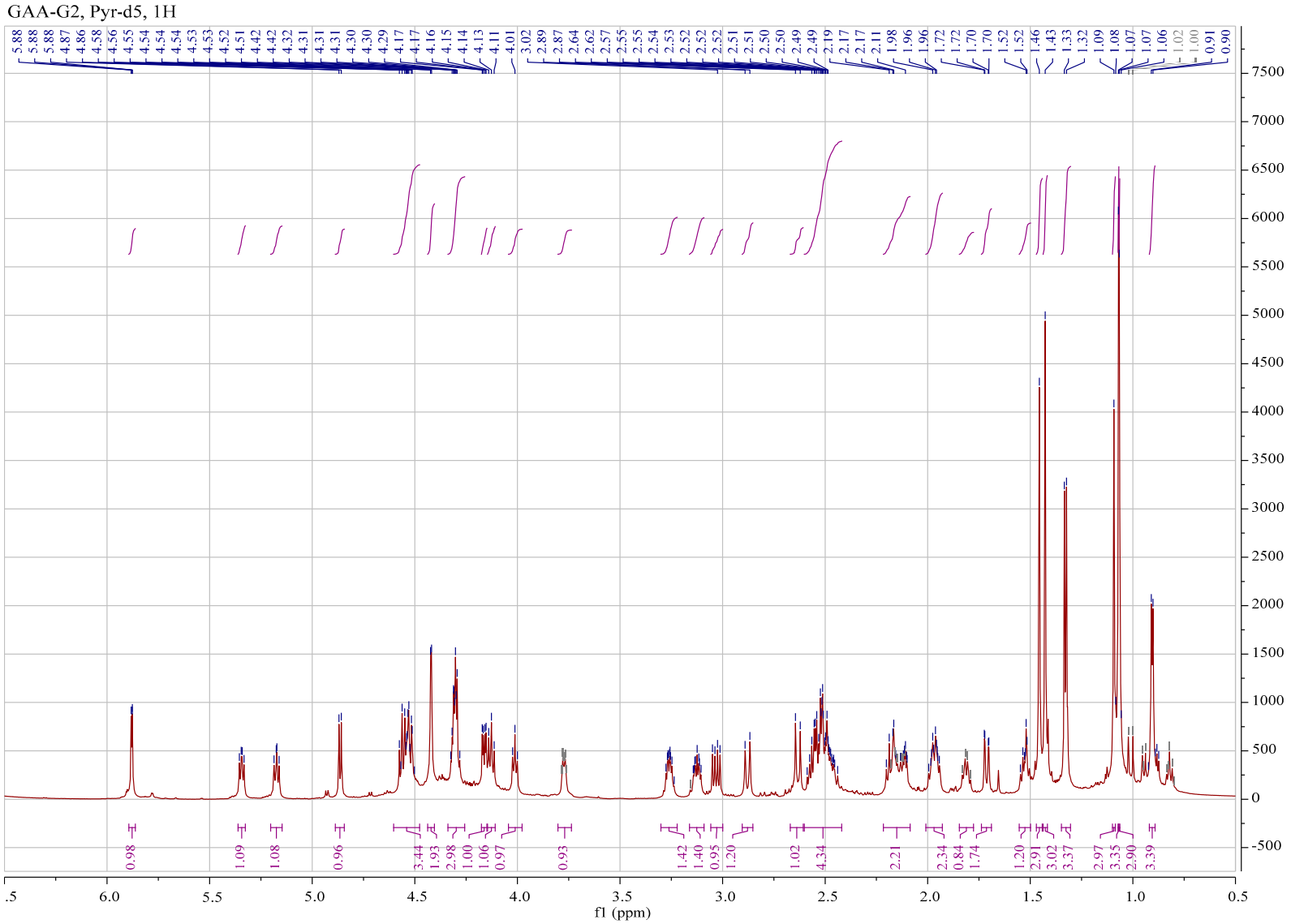

Figure S7. The ^{1}H-NMR (700 MHz) spectrum of GAA-G2 in pyridine-d5.

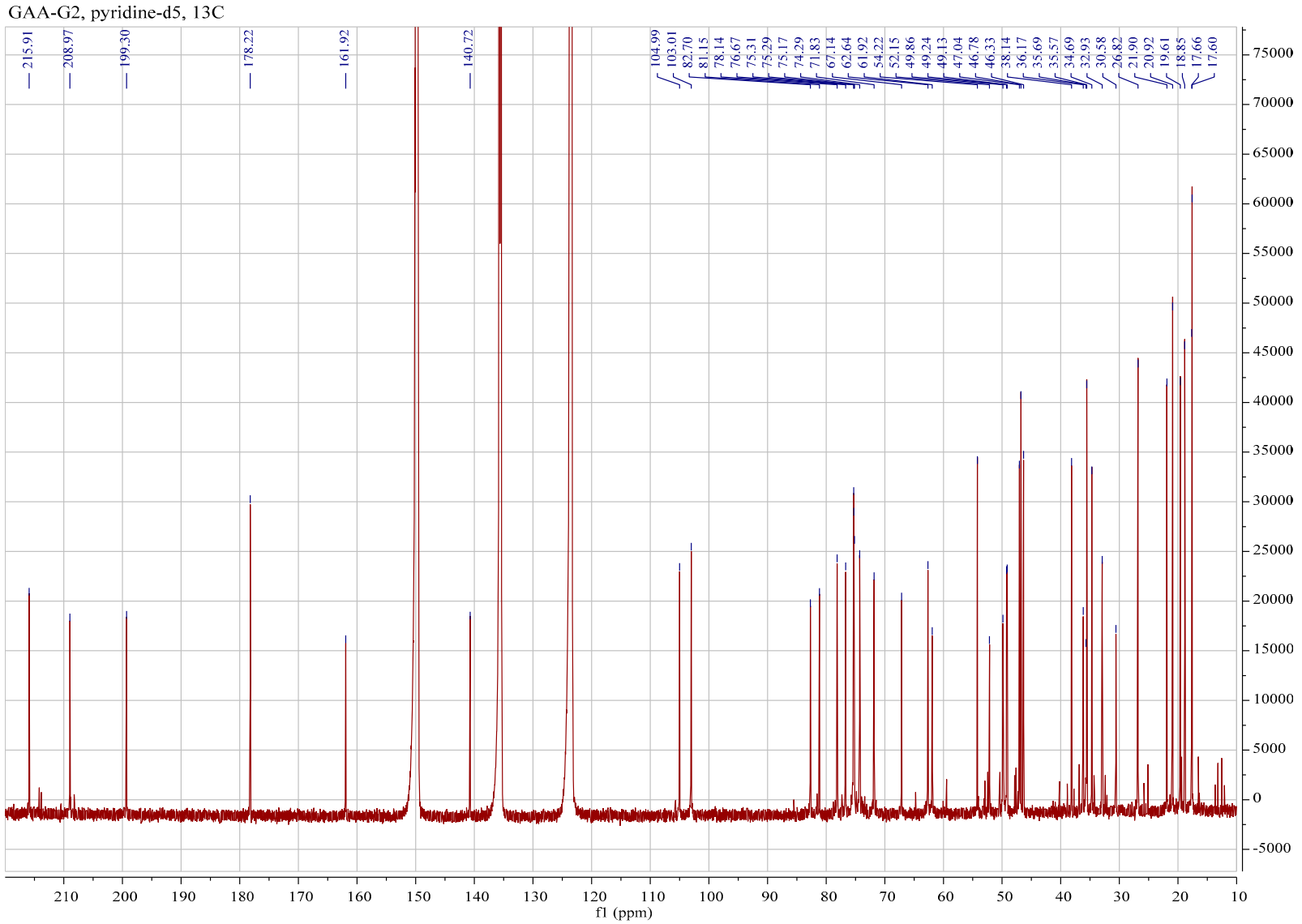

Figure S8. The ^{13}C-NMR (176 MHz) spectrum of GAA-G2 in pyridine-d5.

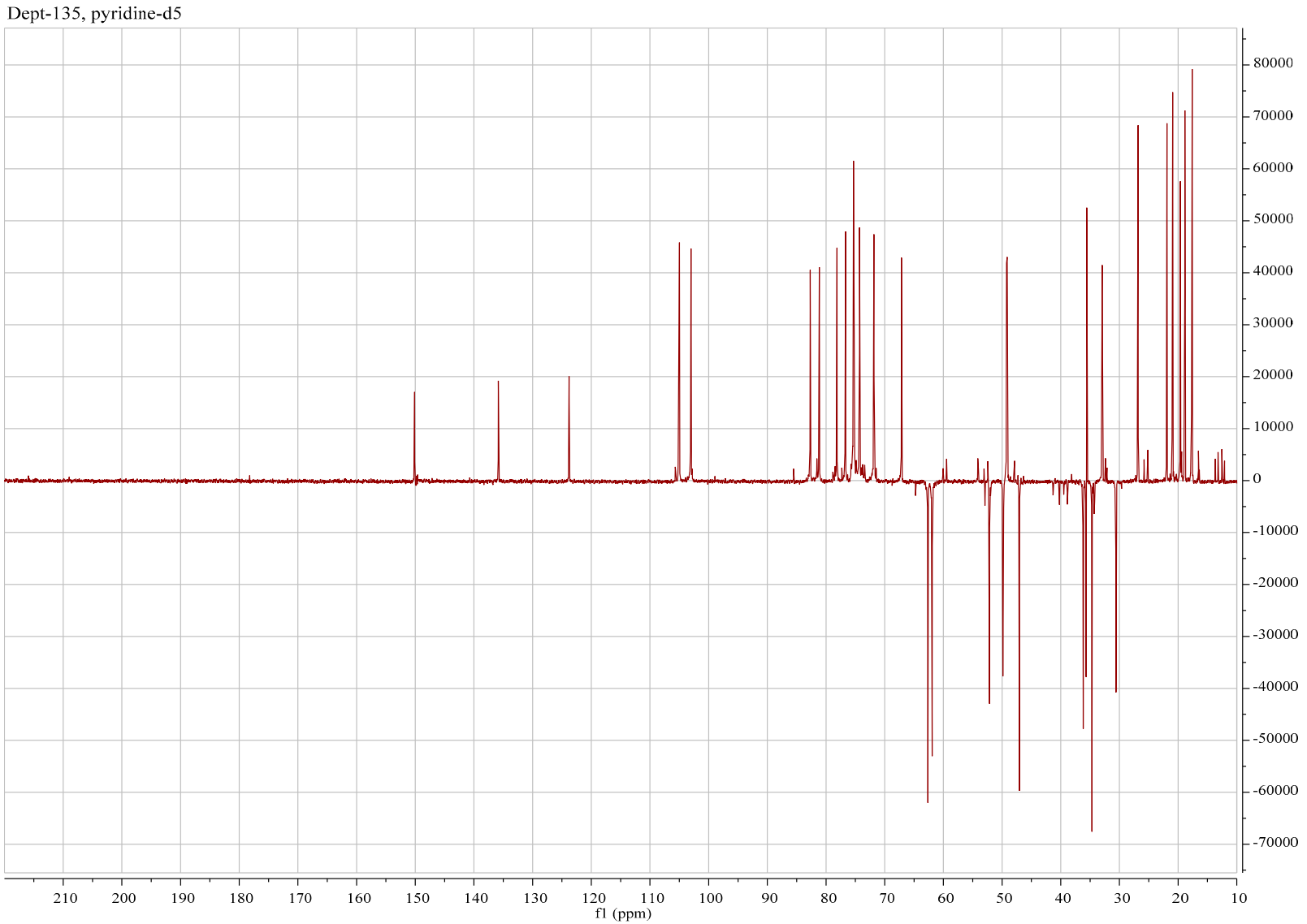

Figure S9. The DEPT-135 (176 MHz) spectrum of GAA-G2 in pyridined-5.

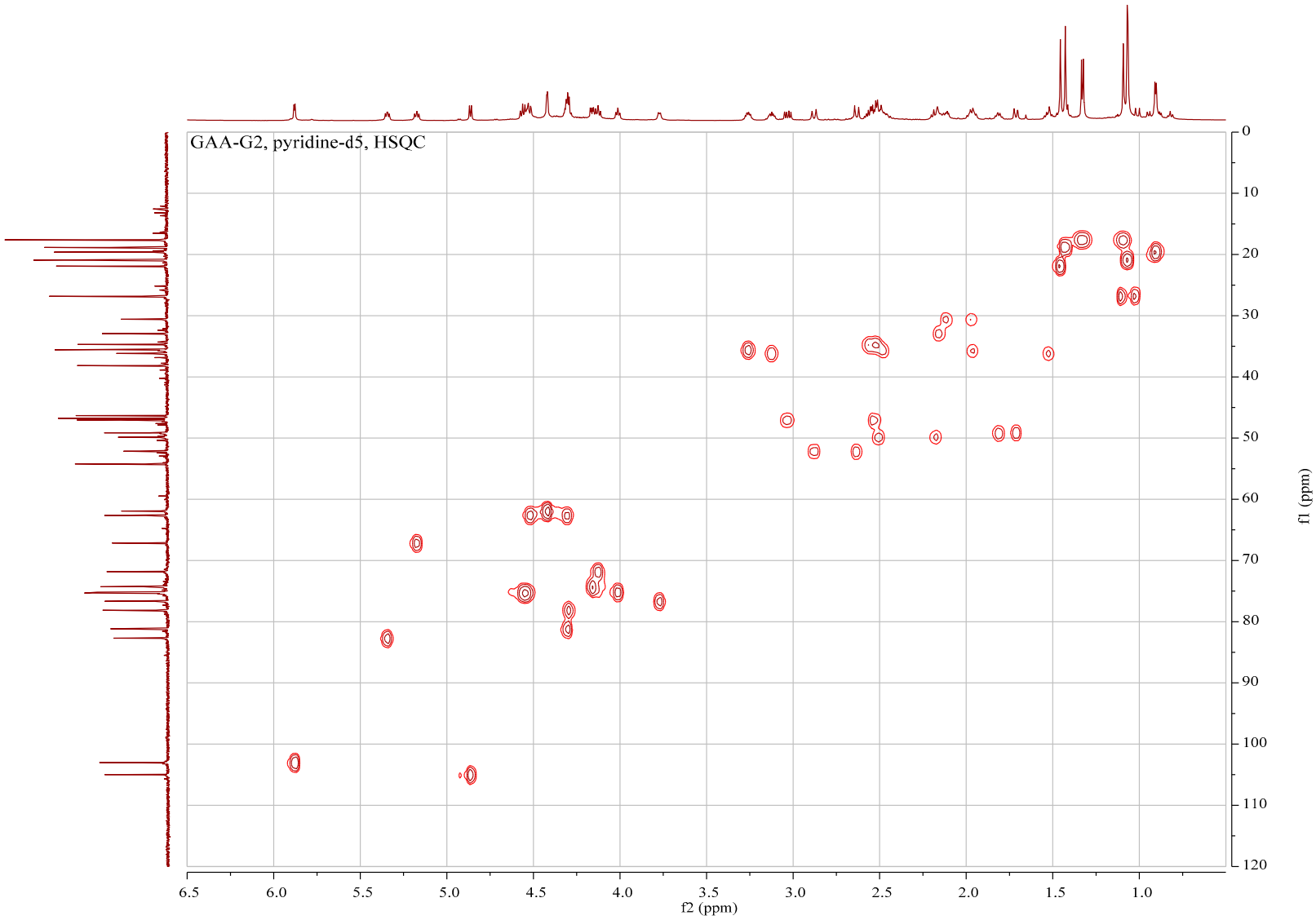

Figure S10. The HSQC (700 MHz) spectrum of GAA-G2 in pyridined-5.

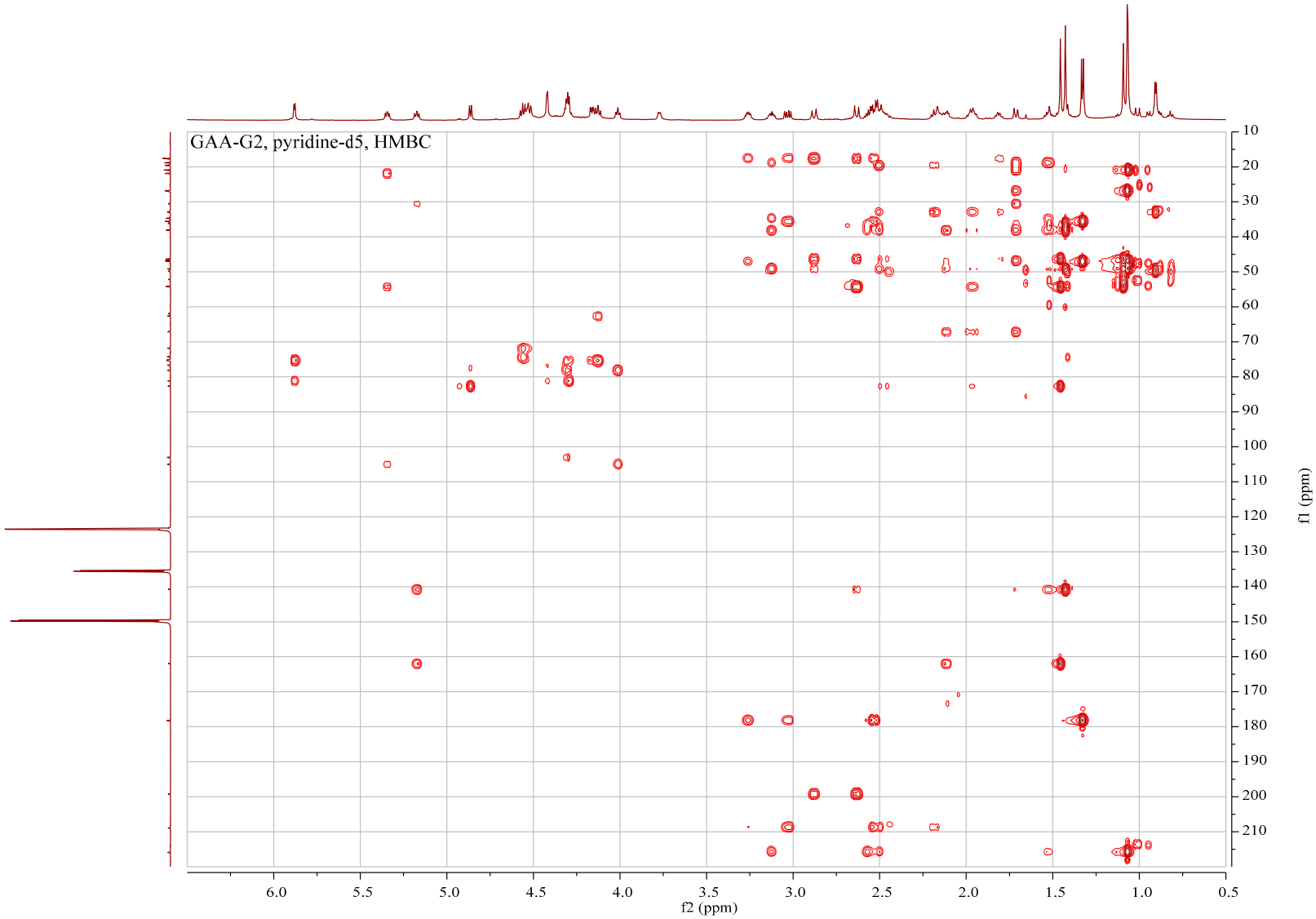

Figure S11. The HMBC (700 MHz) spectrum of GAA-G2 in pyridined-5.

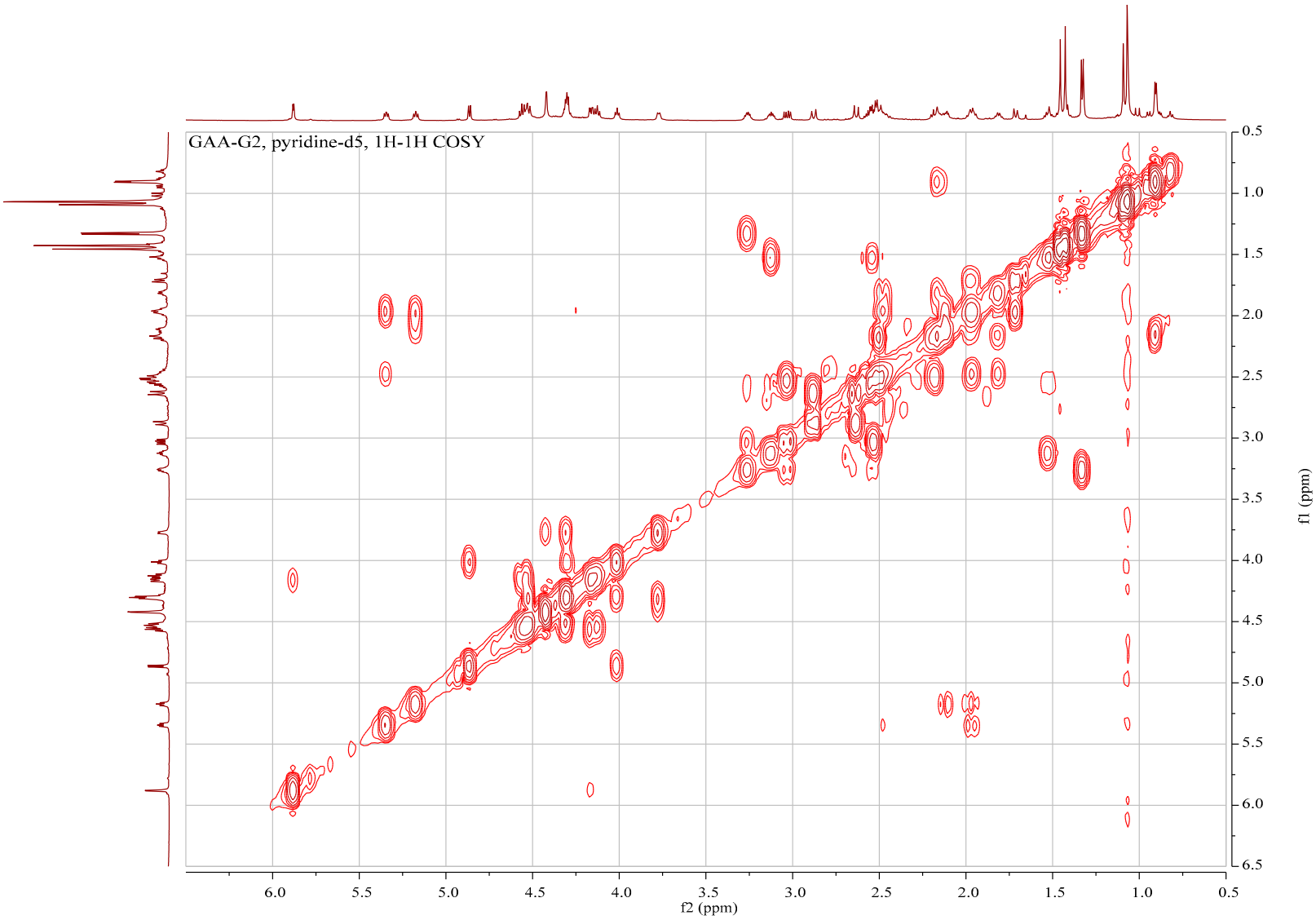

Figure S12. The ^{1}H-^{1}H COSY (700 MHz) spectrum of GAA-G2 in pyridine-d5.

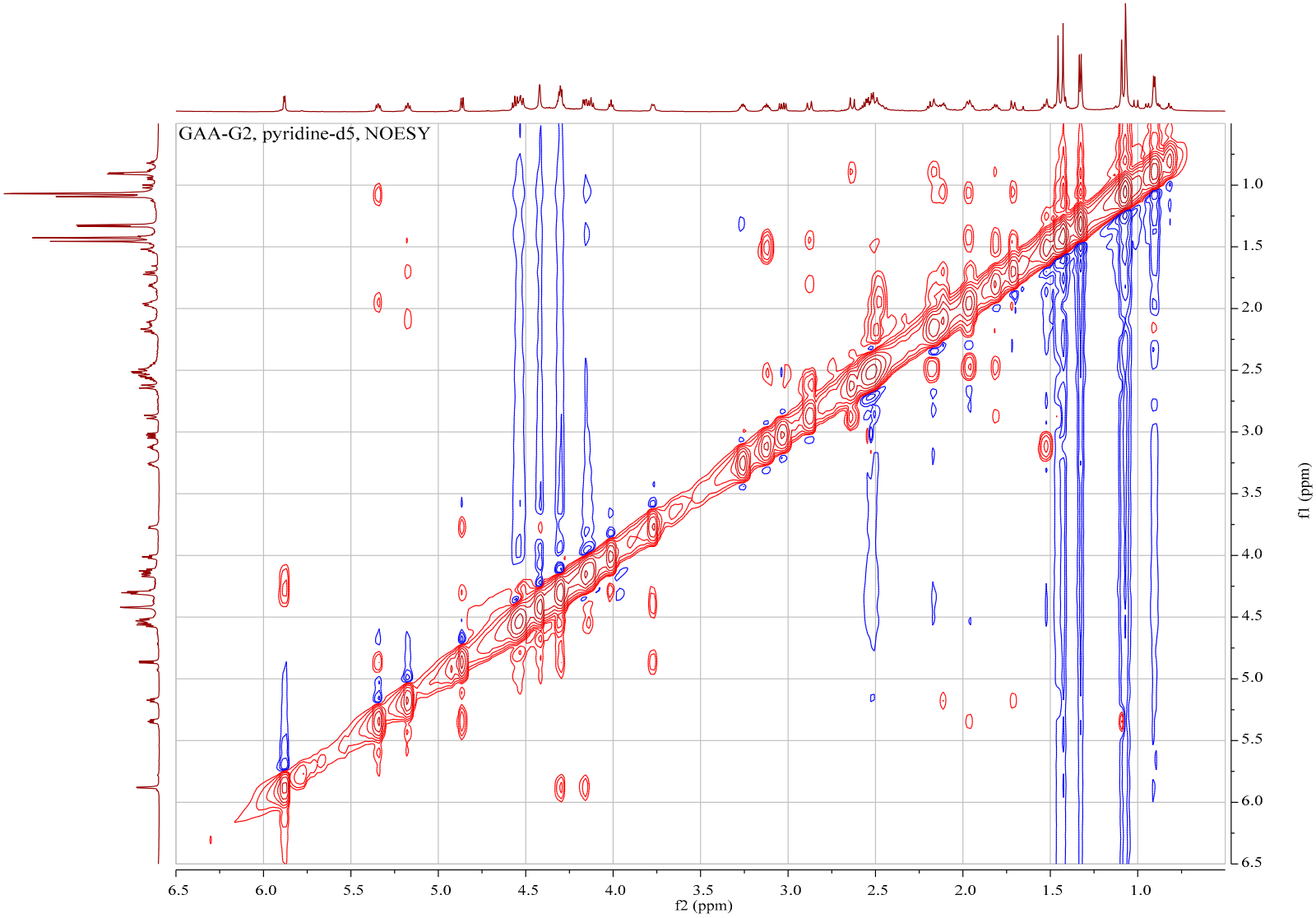

Figure S13. The NOESY (700 MHz) spectrum of GAA-G2 in pyridined-5.